Multiple-Stimuli Responsive Bioelectrocatalysis Based on Reduced Graphene Oxide/Poly(N-isopropylacrylamide) Composite Films and Its Application in the Fabrication of Logic Gates

Lei Wang,[†] Wenjing Lian,[†] Huiqin Yao,[§] and Hongyun Liu*[,†,‡]

[†]College of Chemistry and [‡]Key Laboratory of Theoretical and Computational Photochemistry, Ministry of Education, College of Chemistry, Beijing Normal University, Beijing 100875, People's Republic of China
[§]Department of Chemistry, Ningxia Medical University, Yinchuan 750004, People's Republic of China

Ⓢ *Supporting Information*

ABSTRACT: In the present work, reduced graphene oxide (rGO)/poly(N-isopropylacrylamide) (PNIPAA) composite films were electrodeposited onto the surface of Au electrodes in a fast and one-step manner from an aqueous mixture of a graphene oxide (GO) dispersion and N-isopropylacrylamide (NIPAA) monomer solutions. Reflection−absorption infrared (IR) and Raman spectroscopies were employed to characterize the successful construction of the rGO/PNIPAA composite films. The rGO/PNIPAA composite films exhibited reversible potential-, pH-, temperature-, and sulfate-sensitive cyclic voltammetric (CV) on−off behavior to the electroactive probe ferrocenedicarboxylic acid ($Fc(COOH)_2$). For instance, after the composite films were treated at −0.7 V for 7 min, the CV responses of $Fc(COOH)_2$ at the rGO/PNIPAA electrodes were quite large at pH 8.0, exhibiting the on state. However, after the films were treated at 0 V for 30 min, the CV peak currents became much smaller, demonstrating the off state. The mechanism of the multiple-stimuli switchable behaviors for the system was investigated not only by electrochemical methods but also by scanning electron microscopy and X-ray photoelectron spectroscopy. The potential-responsive behavior for this system was mainly attributed to the transformation between rGO and GO in the films at different potentials. The film system was further used to realize multiple-stimuli responsive bioelectrocatalysis of glucose catalyzed by the enzyme of glucose oxidase and mediated by the electroactive probe of $Fc(COOH)_2$ in solution. On the basis of this, a four-input enabled OR (EnOR) logic gate network was established.

KEYWORDS: reduced graphene oxide, poly(N-isopropylacrylamide), multiple-stimuli responsive, bioelectrocatalysis, logic gates
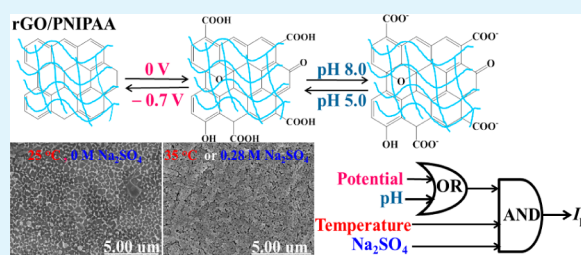
1. INTRODUCTION

In recent years, switchable bioelectrocatalysis based on a combination of enzymatic reactions and stimuli-responsive films that are modified on the electrode surface has attracted considerable attention among researchers because it can offer a model to better comprehend the activation/deactivation mechanism of enzymatic reactions in real biological systems and can be used to fabricate switchable and tunable biofuel cells, biosensors, and other bioelectronic devices.[1−3] A variety of external stimuli have been applied in this area, such as the pH,[4] temperature,[5] electric field,[6] magnetic field,[7] and light.[8] Herein, the multiple-stimuli responsive bioelectrocatalysis systems[9−12] have extraordinary advantages over the single-stimulus triggered ones since the addition of new stimuli or dimensions causes the system to become more complicated, making it similar to real biological systems. In addition, on the basis of the multiple-stimuli sensitive bioelectrocatalysis, more elaborate logic-gate networks could be established, which would be helpful to realize information transduction/amplification and to solve some biomedical problems,[13] as well as to achieve data processing/storage at the nanometer-sized or even molecular levels in chemical/biomolecular computing.[1,14]

The general strategy to construct multiple-stimuli responsive films is to couple various single-stimulus sensitive components or constituents together. For example, copolymer[15] and semi-interpenetrating polymer network (semi-IPN)[9] films with two stimulus-sensitive polymer components were fabricated on an electrode surface by our group, and based on these, multiresponsive bioelectrocatalysis was realized. However, as we know, the multiple stimuli-sensitive electrochemistry system based on graphene or its derivatives has not been reported until now.

Graphene oxide (GO), which is regarded as one of the most significant derivatives of graphene, has aroused great interest recently due to its outstanding thermal, electronic, and mechanical properties as well as its potential value in applications.[16,17] Because GO has plenty of hydrophilic

oxygenated groups, it can be facilely dispersed in water.[18] Thus, GO is often used as a building block or precursor for synthesizing various functional materials.[16,17] GO has also been used to prepare pH-sensitive materials because the protonation/deprotonation of carboxylic acid groups on the GO surface can be controlled by using different pH levels in solution.[19−22] In particular, GO could be easily reduced into its reduced form (rGO) on the electrode surface by electrochemistry.[23,24] We thus expected that the number of oxygenated groups of GO and the corresponding states of the graphene derivatives (GO or rGO) at the electrodes should be easily modulated by different applied potentials. However, the potential-responsive switch based on GO-related system has not been reported until now.

Poly(N-isopropylacrylamide) (PNIPAA), as a model of the thermosensitive polymers, is usually used to prepare thermo- and anion-triggered materials.[5,25] PNIPAA experiences a phase transition at its lower critical solution temperature (LCST) of ~32 °C in water solution.[26,27] Below the LCST, PNIPAA has a swollen structure in solution mainly owing to the absorption of large amounts of water. Above the LCST, the PNIPAA network collapses and has a contracted structure because of the destruction of the hydrogen bonding interaction between PNIPAA networks and water molecules, while the intra- and intermolecular hydrophobic interactions within PNIPAA become predominant. Recently, various GO/PNIPAA or rGO/PNIPAA composite hydrogel materials were prepared, and their temperature-sensitive properties were investigated.[28−33] However, in these studies, GO or rGO did not act as the stimulus-sensitive component. For example, Ye and co-workers prepared PNIPAA/SA/GO hydrogel with pH- and thermoresponsive property, where SA represents sodium alginate.[30] However, GO in the hydrogel only functioned as a cross-linker, while SA was the pH-sensitive component in the composite.

In this work, rGO/PNIPAA thin films were electrodeposited onto the surface of Au electrodes. After cyclic voltammetric (CV) scans in the aqueous dispersion of GO sheets and N-isopropylacrylamide (NIPAA) monomers, NIPAA was electropolymerized into PNIPAA on the electrode surface, and GO was entrapped into the PNIPAA networks and transferred to rGO. The potential-, pH-, temperature-, and SO_4^{2-}-responsive electrochemical behaviors of the electroactive probe Fc-$(COOH)_2$ at the rGO/PNIPAA electrodes was realized, where the $Fc(COOH)_2$ represents ferrocenedicarboxylic acid. The pH- and potential-responsive behavior originated from the rGO constituent, and the temperature- and SO_4^{2-}-responsive property was from the PNIPAA component. This multistimuli responsive CV property of $Fc(COOH)_2$ at the rGO/PNIPAA electrodes could be further employed to modulate the oxidation of glucose electrocatalyzed by GOx and mediated by Fc-$(COOH)_2$ in solution, where GOx represents glucose oxidase. The multiple-stimuli responsive bioelectrocatalysis system was also employed to fabricate the distinctive four-input enabled OR (EnOR) logic gate circuit. As we know, this work is the first study reporting the multiply switchable bioelectrocatalysis on the basis of graphene derivatives. The present study may provide a new possibility for the application of GO/rGO and open up a novel avenue toward the development of multiresponsive biosensors and logic gate networks.

2. EXPERIMENTAL SECTION

2.1. Chemicals. Glucose oxidase (GOx, E.C. 1.1.3.4, type VII from *Aspergillus niger*, 192 000 units g^{-1}), ferrocene methanol (FcOH), methylene blue (MB), and N,N-methylenebis(acrylamide) (BIS) were obtained from Sigma−Aldrich (Shanghai). N-isopropylacrylamide (NIPAA) and 1,1-ferrocenedicarboxylic acid ($Fc(COOH)_2$) were obtained from TCI. Graphite was bought from Tianjin BoDi Co. $Na_2S_2O_8$ was from Aladdin Reagents. Potassium permanganate ($KMnO_4$) was purchased from Tianjin Haiguang Chemical Plant. The other chemicals were all of analytical grade and used as received. The Britton−Robinson buffers containing 0.1 M NaCl were used as buffer solutions from pH 5.0 to 9.0. Solutions were prepared with ultrapure water purified with a Millipore purification system (18.2 MΩ cm).

2.2. Preparation of Graphene Oxide. Graphene oxide was prepared from graphite with the modified Hummers method.[34] In brief, graphite powder (5 g) and 2.5 g of $NaNO_3$ were placed into 115 mL of concentrated H_2SO_4 in a beaker at 0 °C. $KMnO_4$ (15 g) was added gradually with powerful stirring under 20 °C. After it was stirred for 2 h, 230 mL of water was slowly added into the mixture. The temperature of the mixture was rapidly increased to 98 °C, and then, the brown yellow suspension was allowed to react further for 30 min. Then, 700 mL of water and 50 mL of a 30% H_2O_2 solution were slowly added in 15 min to terminate the reaction. The yellow-brown graphite oxide was washed with a dilute HCl solution, and its dispersion was then dialyzed to remove the acids and metal ions completely. Twenty milliliters of the dispersion was dried at 40 °C for 36 h, and then, the graphite oxide was obtained. A certain amount of graphite oxide was dispersed and exfoliated in a pH 5.0 buffer by ultrasonication for 3 h to obtain a homogeneous and stable dispersion of GO, which was then stored in the refrigerator at 4 °C. The characterization of GO was performed using various techniques, which are described in detail in the Supporting Information.

2.3. Preparation of rGO/PNIPAA Composite Films. The Au disk electrodes (ϕ = 2 mm, from CH Instruments) were polished and cleaned according to the previously reported method.[5] For the electrodeposition of composite films on Au electrodes, a typical precursor solution containing 0.1 mg mL^{-1} GO dispersion, 0.8 M NIPAA, 0.01 M initiator $Na_2S_2O_8$, 2 mg mL^{-1} cross-linker BIS, and 0.15 M $NaNO_3$ was adopted after optimization. The electrodeposition was performed in a nitrogen-saturated atmosphere with CV scans between −0.1 and −1.3 at 0.1 V s^{-1} for 20 cycles. In the procedure, not only was NIPAA polymerized into PNIPAA but also GO was entrapped into the PNIPAA films and electrochemically reduced to rGO. After the electrodeposition, the rGO/PNIPAA film electrodes were flushed with pure water to remove the unreacted chemicals. The pure PNIPAA films were also electropolymerized onto the Au electrode surface using the same method, except that there was no GO in the precursor solution.

2.4. Apparatus and Procedures. All of electrochemical tests were carried out on a CHI 660A electrochemical workstation, using a three-electrode cell system with a platinum foil as the counter electrode, a saturated calomel electrode (SCE) as the reference electrode, and the modified Au electrode as the working electrode. CVs were usually performed at rGO/PNIPAA film electrodes between 0.1 and 0.8 V at the rate of 0.1 V s^{-1} under different conditions in 0.05 mM $Fc(COOH)_2$ solutions. For bioelectrocatalysis, 1.0 mg mL^{-1} GOx and 6.0 mM glucose were added into the above solutions, and CVs were scanned at 0.01 V s^{-1}. Before CV tests, the high-purity nitrogen was bubbled into the buffers in the cell for more than 15 min. The N_2 environment was then kept during the experiment.

Reflection−absorption infrared (IR) spectra were collected using an IFS-66v/S IR spectrometer (Bruker) at a resolution of 4 cm^{-1}. Raman analyses were carried out on a Raman spectrometer (Jobin Yvon) equipped with a He−Ne laser emitting 632.8 nm wavelength light. The PNIPAA and rGO/PNIPAA films electrodeposited onto indium tin oxide (ITO) electrodes were used as the samples for the IR and Raman measurements.

Scanning electron microscopy (SEM) was performed using an X-650 scanning electron microanalyzer (Hitachi) operating at 5.0 kV. The rGO/PNIPAA films electrodeposited onto gold-film modified quartz crystal disks were served as samples for SEM tests. After they were exposed to different Na_2SO_4 solutions, temperature, and pH for 5 min, the samples were immediately placed into liquid N_2 to make the structure "frozen". Afterward, the samples were placed in a lyophilizer (Boyikang, Beijing) for 24 h to remove all of the water in the composite films. The samples were coated by a thin platinum layer using an E-1045 sprayer (Hitachi) before SEM tests.

X-ray photoelectron spectroscopy (XPS) was performed using an ESCSLAB 250Xi X-ray photoelectron spectrometer (Thermo Fisher) equipped with a monochromatized Al Kα radiation source (2721 eV). The PNIPAA, rGO/PNIPAA, and rGO films electrodeposited onto ITO electrode surfaces were used as the samples.

3. RESULTS AND DISCUSSION

3.1. Characterization of rGO/PNIPAA Films.

The formation of PNIPAA by the electropolymerization of NIPAA monomers at the Au electrodes using CV was reported previously[5,35] and was also confirmed by the IR spectra in the present work (Figure S1 and Table S1 in the Supporting Information). The absorption peak of the C=C vibration at 1625 cm^{-1} for NIPAA was not found for the PNIPAA films, indicating that the NIPAA was successfully electropolymerized into PNIPAA. For rGO/PNIPAA films, while the IR results could not provide direct evidence for the formation of PNIPAA due to the interference of rGO in the films, the formation of PNIPAA during electrodeposition should be certain and positive. The network architecture observed using SEM and the thermosensitive property observed using SEM and CV for the films provided strong supporting evidence for the formation of PNIPAA in the rGO/PNIPAA films, which will be described and discussed in detail in subsection 3.5.

The entrapment of GO into PNIPAA networks and the reduction of GO into rGO in the rGO/PNIPAA films were confirmed by IR (Figure S1 and Table S1) and Raman spectroscopy (Figure 1). The typical IR absorption peaks of
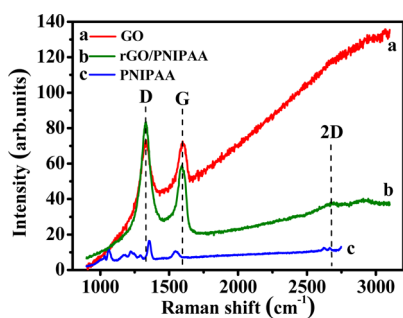

Figure 1. Raman spectra of the (a) GO, (b) rGO/PNIPAA, and (c) PNIPAA samples.

$\nu_{C=C}$, $\nu_{C=O}$, and ν_{C-O} at 1620, 1728, and 1054 cm^{-1} for GO, respectively, were also found in the rGO/PNIPAA samples, suggesting that GO is successfully entrapped into the PNIPAA films.

The Raman peak at 1580 cm^{-1}, which was ascribed to the G-band from the vibration of sp^2-bonded carbon in the graphene skeleton,[36] and the peak at 1350 cm^{-1}, which was ascribed to the disorder-related D-band from the breathing mode of A$_{1g}$ symmetry of sp^3 carbon,[37,38] were observed for both the GO and rGO/PNIPAA samples. Meanwhile, for the pure PNIPAA samples, the Raman absorption peaks in the same range were

very weak under the same condition (Figure 1). These results imply that the GO is successfully electrodeposited into PNIPAA films. The D/G intensity ratio for rGO/PNIPAA (1.83) was obviously higher than that for GO (1.19), suggesting the reduction of the GO in the composite films.[23,39] In addition, a weak two-dimensional peak at 2700 cm^{-1} was observed for the rGO/PNIPAA samples but was not detected for GO, also supporting the reduction of GO into rGO in the films.[23] All of these results suggest that during the electrodeposition, GO not only is entrapped into PNIPAA films but also mainly takes the reduced form of GO (rGO) in the films.

3.2. Potential-Controlled Cyclic Voltammetric Behavior of Fc(COOH)₂ for rGO/PNIPAA Films.

The potential applied on the rGO/PNIPAA films had a significant effect on the film properties and the CV signal of the electroactive probe $Fc(COOH)_2$ at rGO/PNIPAA composite film modified electrodes. First, the influence of different applied potentials and applied time on the CV response of $Fc(COOH)_2$ was explored (Figure S3 in the Supporting Information). After optimization, −0.7 and 0 V were chosen as two typical potentials to study the potential-sensitive electrochemical property of $Fc(COOH)_2$ at the rGO/PNIPAA film electrodes. After treatment at −0.7 V for 7 min in pH 7.0 buffers, the rGO/PNIPAA film electrode was transferred into pH 8.0 buffer solutions in the presence of $Fc(COOH)_2$. CV was then performed between 0.1 and 0.8 V at 0.1 V s^{-1} and 25 °C. A couple of quasi-reversible CV peaks were observed at ∼0.42 V with relatively large peak currents (Figure 2, curve b), which is
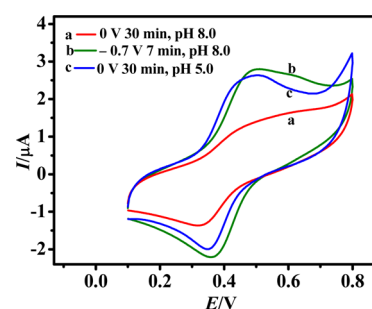

Figure 2. CVs of 0.5 mM Fc(COOH)₂ for rGO/PNIPAA films at 0.1 V s^{-1} and 25 °C (a) in pH 8.0 buffers after the films were treated at 0 V for 30 min, (b) in pH 8.0 buffers after the films were treated at −0.7 V for 7 min, and (c) in pH 5.0 buffers after the films were treated at 0 V for 30 min.

characteristic of the ferrocene redox couple. However, after the film electrode was treated at 0 V for 30 min in pH 7.0 buffers and then placed into the pH 8.0 buffers containing $Fc(COOH)_2$, the CV peak currents became much smaller (Figure 2, curve a). If the CV oxidation peak (I_{pa}) of $Fc(COOH)_2$ at the film electrode after treatment at −0.7 V was defined as the on state and the I_{pa} for the films treated at 0 V was defined as the off state, then the system demonstrated potential-sensitive on−off property. This switchable behavior was found to be reversible. When the potential was switched between −0.7 and 0 V, the corresponding CV I_{pa} of the probe could transform between the on and off states several times in pH 8.0 solutions (Figure 3A).

The control experiments were performed to test the possibility whether the probe exhibited similar potential-sensitive CV on−off behaviors for PNIPAA films under the
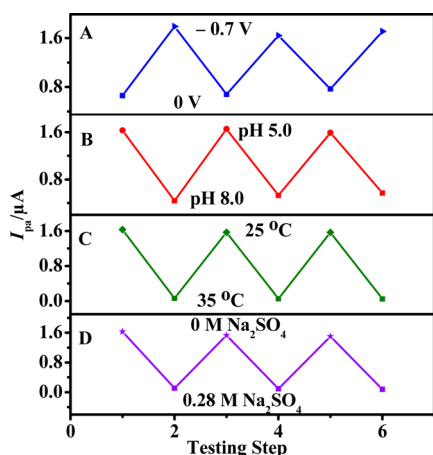
Figure 3. Dependence of I_{pa} of 0.5 mM Fc(COOH)$_2$ at 0.1 V s^{-1} for rGO/PNIPAA films on (A) the potential switched between −0.7 and 0 V at pH 8.0 and 25 °C, (B) the solution pH switched between 5.0 and 8.0 at 25 °C after the film electrodes were treated at 0 V for 30 min, (C) the solution temperature switched between 25 and 35 °C at pH 5.0, and (D) the Na$_2$SO$_4$ concentration cycled between 0 and 0.28 M at pH 5.0 and 25 °C.

same conditions. The probe in the pH 8.0 solution exhibited almost the same CV peak potentials and currents after the PNIPAA film electrodes were treated at −0.7 and 0 V (Figure S4 in the Supporting Information), indicating that the potential-sensitive CV property of Fc(COOH)$_2$ for rGO/PNIPAA films should be ascribed to the rGO component in the films.

3.3. pH-Responsive Behavior of Fc(COOH)$_2$ at rGO/PNIPAA Film Electrodes. After treatment at 0 V for 30 min, the rGO/PNIPAA films exhibited a pH-responsive behavior toward Fc(COOH)$_2$. In pH 8.0 buffers, the CV peak currents of Fc(COOH)$_2$ were very small (Figure 2, curve a). However, in pH 5.0 solutions, the CV peak currents became fairly large (Figure 2, curve c), similar to those for the films treated at −0.7 V for 7 min and then tested by CV at pH 8.0 (Figure 2, curve b). The CV I_{pa} of the probe at the rGO/PNIPAA film electrodes exhibited a decreasing trend with the increase of solution pH from pH 5.0 to 9.0, and the peak potential difference (ΔE_p) increased correspondingly (Figure 4), indicating that Fc(COOH)$_2$ diffuses through the rGO/PNIPAA films with more difficulty when the solution pH increases. If, after the rGO/PNIPAA film electrodes were
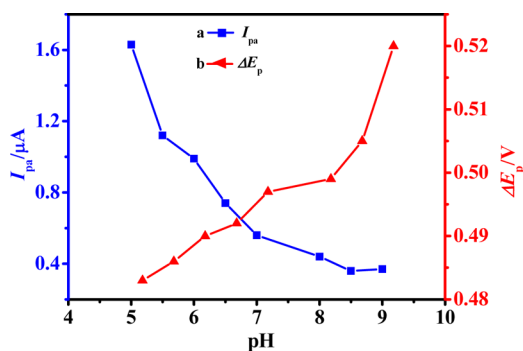
treated at 0 V, the I_{pa} was considered as the on state at pH 5.0 and as the off state at pH 8.0, then this pH-responsive switching behavior could be duplicated many times with a response time of less than 1 min (Figure 3B), suggesting that the pH-responsive property of the system is reversible.

The control experiments were designed to investigate whether the probe exhibited a similar pH-sensitive CV behavior at bare Au or PNIPAA film electrodes under the same conditions. The probe exhibited almost the same CV peak positions and heights between pH 5.0 and 8.0 with very similar CV shapes at either bare Au or PNIPAA film electrodes after the electrodes were treated at 0 V for 30 min (Figure S5 in the Supporting Information), indicating that the pH-responsive behavior for the rGO/PNIPAA film system should be caused by the rGO constituent in the films.

3.4. The Mechanism Study. Two representative mechanisms are usually used to explain the pH-responsive CV property of electroactive probes at the film modified electrodes: (1) the film structure is responsive to the surrounding pH and changes along with the solution pH;[40] (2) the electrostatic attraction/repulsion between the probes and films is sensitive to the surrounding pH.[41,42] To test the first possibility for the present system, SEM was used to examine the rGO/PNIPAA films after the films dealt with 0 V for 30 min and then with different pH. After the rGO/PNIPAA films were immersed into pH 5.0 and 8.0 buffers for 5 min and then dried, respectively, SEM examination of the films revealed very similar surface morphologies (Figure 5A,B), suggesting that the change of
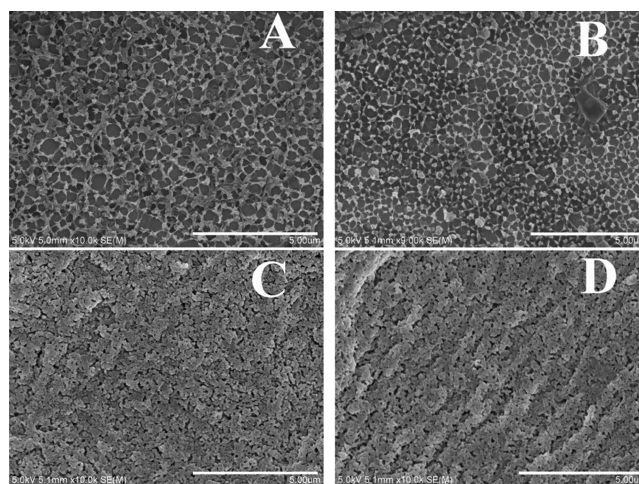

Figure 5. Top-view SEM images of rGO/PNIPAA films after treatment at 0 V for 30 min, then by successive treatment with (A) pH 5.0 buffers at 25 °C, (B) pH 8.0 buffers at 25 °C, (C) pH 5.0 buffers at 35 °C, and (D) pH 5.0 buffers containing 0.28 M Na$_2$SO$_4$ at 25 °C.

Figure 4. Effect of the solution pH on (a) I_{pa} and (b) ΔE_p of 0.5 mM Fc(COOH)$_2$ at 25 °C and 0.1 V s^{-1} for rGO/PNIPAA films after treatment at 0 V for 30 min.

solution pH cannot cause the significant structural change of the films with the current magnification. Thus, the second mechanism is most probably responsible for the pH-sensitive property of the system.
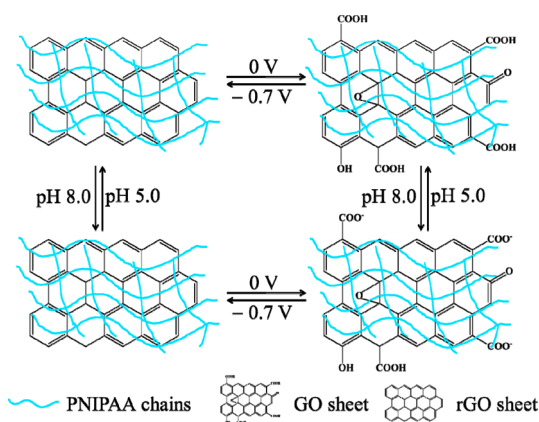
After treatment at 0 V for 30 min, the rGO in the rGO/PNIPAA films is oxidized to GO with more oxygen-containing functional groups, such as phenolic hydroxyl and carboxylic acid groups on the surface. On one hand, under the condition of pH above 5.0, Fc(COOH)$_2$ becomes ionized and always carries negative charges.[43,44] At pH 8.0, the GO carries negative charges due to the deprotonation of the carboxylic acid

groups.[45] Thus, the electrostatic repulsion between the negatively charged GO in the films and the similarly charged probe in buffers would lead to the difficulty of the $Fc(COOH)_2$ to diffuse into the films and transfer electrons with the electrodes, leading to the very small peak currents. On the other hand, in pH 5.0 solutions, the more acidic pH environment is unfavorable to the ionization of the −COOH groups on the GO surface. The GO in the films carries less or even no negative charges at this pH. The electrostatic repulsion between GO in the films and $Fc(COOH)_2$ in solution thus would become very weak, and the probe could pass through the rGO/PNIPAA films much more easily, leading to a lager CV signal. This mechanism was also confirmed by the CV measurements of differently charged probes (neutral FcOH, positively charged MB, and negatively charged $Fe(CN)_6^{3-}$) at different pH values for rGO/PNIPAA films after the films were treated at 0 V for 30 min (Figure S6 in the Supporting Information). The electrostatic attraction/repulsion between the GO in the composite films and $Fc(COOH)_2$ at different pH is thus responsible for the pH-responsive CV behavior of the system.

The electrostatic interaction between the probe and the films could also be used to interpret the mechanism of the potential-sensitive CV property of this system. After treatment at 0 V for 30 min, the rGO in the rGO/PNIPAA films is oxidized to GO, and its charge situation becomes sensitive to the solution pH, as discussed above. However, after treatment at −0.7 V for 7 min, the GO in the films is reduced back to rGO. The amount of phenolic hydroxyl and carboxylic acid groups on the GO surface thus become very limited, and the rGO in the films becomes neutral and carries no charge at any pH. The electrostatic repulsion between the rGO in rGO/PNIPAA films and the probe in solution becomes very weak. This explains why the probe could diffuse into the films more easily and then exchange electrons with the electrode more smoothly after the films were treated at −0.7 V, leading to the lager CV response or the on state, even at pH 8.0, while, in the same pH 8.0 solution, the system exhibited the off state after the films were treated at 0 V (Figures 2 and 3A). The mechanism of the pH- and potential-responsive behavior of the system is schematically illustrated in Scheme 1.

The above explanation for the potential-sensitive CV behavior of the system was further supported by the XPS results (Figure S7 in the Supporting Information). The oxygen/

carbon (O/C) atomic ratio from the XPS spectra for electrodeposited PNIPAA, rGO/PNIPAA, and rGO films after the films were treated at −0.7 and 0 V is listed in Table 1. The rGO films after treatment at 0 V for 30 min exhibited a

Table 1. O/C Ratio Extracted from the High-Resolution XPS Spectra and the C(O)/C(C) Ratio from the C 1s XPS Spectra for rGO, rGO/PNIPAA, and PNIPAA Films after the Treatment at Different Potentials

	O/C		C(O)/C(C)	
sample	0 V	−0.7 V	0 V	−0.7 V
rGO	0.492	0.370	1.46	0.997
rGO/PNIPAA	0.392	0.331	0.744	0.626
PNIPAA	0.243	0.279	0.177	0.178

much higher O/C ratio than that of the same films after treatment at −0.7 V for 7 min, suggesting that the majority of rGO is oxidized into GO in the films after the films are treated at 0 V and that the state of graphene derivatives (rGO or GO) in the films can be modulated by applied potentials.[23] The same trend and the similar situation were also observed for rGO/PNIPAA films, but the difference of the O/C ratio between 0 and −0.7 V for the rGO/PNIPAA films was not as obvious as that for the rGO films. This result is understandable because the PNIPAA films after treatment at 0 V exhibited a smaller O/C ratio than the same films after treatment at −0.7 V. The detailed XPS spectra in the C 1s range are shown in Figure S8 in the Supporting Information. The ratio of C(O)/C(C) for different films treated at different potentials is also listed in Table 1, where C(C) represented the sum of peak area centered at 284.8 eV (C=C) and 285.5 eV (C−C), while C(O) denotes the sum of the peak area at 286.2 eV (C−O), 286.9 eV (C=O), and 288.3 eV (C(O)O).[46] The assignment of these XPS peaks for the rGO samples after treatment at 0 V is shown in Figure S8A, as an example. In brief, C(O) represents the amount of carbon bonded with oxygen, and C(C) represents the amount of carbon bonded with carbon. The ratio C(O)/C(C) for the rGO films after treatment at 0 V was obviously larger than that for the films treated at −0.7 V because of the oxidation of rGO. For the rGO/PNIPAA films, the trend was the same, but the difference of the C(O)/C(C) ratio between 0 and −0.7 V was not as obvious as that for the rGO films, which is most likely because of the interference of PNIPAA. All of these XPS results support our speculation that, after treatment at 0 V, the majority of rGO in the rGO/PNIPAA films is oxidized to GO, while after treatment at −0.7 V, most of these GO sheets are reduced back to rGO.

The CV of $Fc(COOH)_2$ at the rGO/PNIPAA film electrodes without potential treatment did not exhibit any pH-sensitive behavior (Figure S9 in the Supporting Information), implying that the majority of rGO in the films indeed takes the reduced form of GO. The result is in agreement with those of the IR (Figure S1), Raman (Figure 1), and XPS analyses (Figure S8C).

3.5. Thermo- and Salt-Responsive Cyclic Voltammetric Property of $Fc(COOH)_2$ at rGO/PNIPAA Films. The present system also exhibited reversible thermoresponsive CV behavior at pH 5.0 (Figure 6A). Below 32 °C, the CV signals of $Fc(COOH)_2$ were relatively large, and the I_{pa} remained almost the same high level, whereas above 32 °C, the CV I_{pa} of the probe decreased sharply with the temperature (Figure 6B). The critical phase-transition temperature was observed at ∼32 °C,
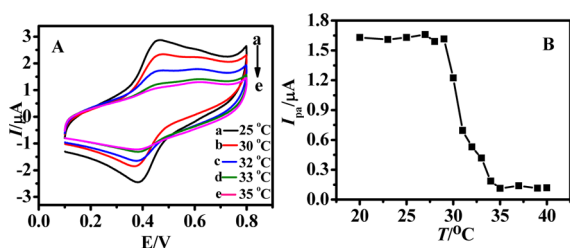
Scheme 1. Charge Situation of rGO/PNIPAA Films at Different pH and Applied Potentials

Figure 6. (A) CVs of 0.5 mM Fc(COOH)$_2$ in pH 5.0 buffers at 0.1 V s^{-1} for rGO/PNIPAA films at (a) 25 °C, (b) 30 °C, (c) 32 °C, (d) 33 °C, and (e) 35 °C. (B) Influence of the solution temperatures on I_{pa} of Fc(COOH)$_2$ in pH 5.0 buffers for the rGO/PNIPAA films.

the same as the LCST for the pure PNIPAA hydrogel.[47] This result suggests that the thermosensitive property of the rGO/PNIPAA films originates from the PNIPAA component but not rGO and that rGO has little effect on the LCST of the PNIPAA films.

According to Figure 6, two representative temperatures, 25 and 35 °C, were chosen to investigate the switching behavior of Fc(COOH)$_2$ for the rGO/PNIPAA films. At 25 °C, Fc-(COOH)$_2$ exhibited quite large CV peaks for rGO/PNIPAA films, showing the on state (Figure 6A, curve a). In contrast, at 35 °C, the probe exhibited the off state, with a very small CV I_{pa} (Figure 6A, curve e). This temperature-sensitive switching behavior was found to be quite reversible (Figure 3C). By cycling the rGO/PNIPAA film electrode in the Fc(COOH)$_2$ solution between 35 and 25 °C, the corresponding CV I_{pa} could switch between the off and on states many times in only a few tens of seconds.
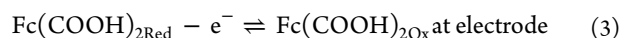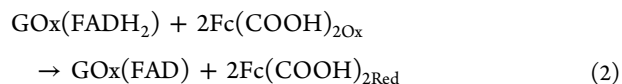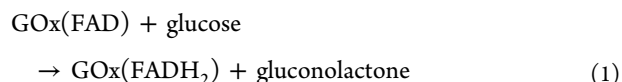
The thermosensitive switching property of the rGO/PNIPAA films to the probe is attributed to the temperature-sensitive structural transformation of the PNIPAA component in the films. Below the LCST, the PNIPAA hydrogel network in the films adopts a swollen state in aqueous solution, mostly owing to the strong hydrogen bonds between amide groups of PNIPAA and the surrounding water molecules.[5,47] Thus, it is easier for Fc(COOH)$_2$ to pass through rGO/PNIPAA films, resulting in the larger CV response. Above the LCST, such as at 35 °C, the PNIPAA network collapses and adopts a contracted structure in aqueous solution due to the destruction of the hydrogen bonding between PNIPAA and water, and the inter- and intramolecular hydrophobic attractions within the PNIPAA networks become predominant.[5,48,49] In this case, it is difficult for the probe to diffuse through the films, resulting in the lower CV response.

The structural transformation of the rGO/PNIPAA films with temperature was also ratified by SEM observations. The surface morphologies of the rGO/PNIPAA films treated at 25 and 35 °C were obviously different (Figure 5A,C). At 25 °C, the films exhibited a network structure with larger-sized holes on the surface. However, at 35 °C, the films exhibited a more contracted structure with much smaller holes.

The CV signal of Fc(COOH)$_2$ for the rGO/PNIPAA films in pH 5.0 solution was also strongly influenced by the type and concentration of the salts in the testing solution (Figure S10 in the Supporting Information). The critical phase transition concentration for various anions was observed with the sequence of Br$^-$ (0.75 M) > Cl$^-$ (0.50 M) > SO$_4^{2-}$ (0.15 M), which is well consistent with the Hofmeister series.[5,50,51] Because SO$_4^{2-}$ exhibited the smallest critical phase transition concentration among the three anions, SO$_4^{2-}$ was chosen as a

representative to investigate the salt-responsive CV on–off behavior of the probe for the rGO/PNIPAA films. When the concentration of SO$_4^{2-}$ switched between 0 and 0.28 M, the CV I_{pa} of the probe cycled between the on and off states reversibly (Figure 3D). The structural change of the rGO/PNIPAA films with SO$_4^{2-}$ concentration was observed using SEM (Figure 5A,D), which was similar to the structural change with temperature. The mechanism of the salt-sensitive property for the films should also be similar to that of the thermosensitive behavior.[5,52] For example, after the addition of 0.28 M Na$_2$SO$_4$ into the pH 5.0 solution, the PNIPAA in the rGO/PNIPAA films adopts a contracted and compact structure. As a result, it was difficult for the Fc(COOH)$_2$ in solution to pass through the rGO/PAIPAA films and arrive at the electrode surface, leading to the off state with a smaller CV response.

3.6. Switchable Bioelectrocatalysis of Glucose by GOx for the System. When a suitable amount of glucose and GOx was injected into Fc(COOH)$_2$ solutions at 25 °C and pH 5.0, the I_{pa} of Fc(COOH)$_2$ at rGO/PNIPAA film electrodes at ~0.45 V increased remarkably compared with that without glucose. At the same time, the reduction peak of the probe decreased or even disappeared. When the concentration of glucose was below 6 mM, the CV I_{pa} increased with the addition of glucose, while, when the glucose concentration was above 6 mM, the I_{pa} leveled off (Figure S11 in the Supporting Information). The results are an obvious indication of the oxidation of glucose electrocatalyzed by GOx and mediated by electroactive Fc(COOH)$_2$:[8,53,54]

$$GOx(FAD) + glucose$$
$$\rightarrow GOx(FADH_2) + gluconolactone \qquad (1)$$

$$GOx(FADH_2) + 2Fc(COOH)_{2Ox}$$
$$\rightarrow GOx(FAD) + 2Fc(COOH)_{2Red} \qquad (2)$$

$$Fc(COOH)_{2Red} - e^- \rightleftharpoons Fc(COOH)_{2Ox} \text{ at electrode} \qquad (3)$$

where GOx(FAD) and GOx(FADH$_2$) denote the oxidized and reduced forms of GOx, respectively, and Fc(COOH)$_{2Red}$ and Fc(COOH)$_{2Ox}$ represent the reduced and oxidized forms of Fc(COOH)$_2$, respectively.

On the basis of the bioelectrocatalysis of glucose, the multiple-stimuli responsive CV switching behavior of Fc-(COOH)$_2$ at the rGO/PNIPAA film electrodes could be greatly amplified. For example, at pH 8.0, after the rGO/PNIPAA film electrode was treated at −0.7 V, the CV I_{pa} of Fc(COOH)$_2$ was very large in the presence of glucose and GOx (Figure 7A, curve a) because the system is at the on state and the bioelectrocatalytic cycle can be realized. However, after the same rGO/PNIPAA film electrode was treated at 0 V, the CV I_{pa} of Fc(COOH)$_2$ for the films became very small (Figure 7A, curve b). This behavior occurred because the diffusion of Fc(COOH)$_2$ through the films becomes difficult, and then the bioelectrocatalytic cycle is interrupted. Hence, the electro-catalytic oxidation of glucose by GOx could be cycled between activation and inactivation states by switching the applied potential between 0 and −0.7 V. If I_{pa}^{on} and I_{pa}^{off} are defined as the CV oxidation peak current at the on and off state, respectively, then the ratio of I_{pa}^{on}/I_{pa}^{off} could be amplified by the bioelectrocatalysis. In the presence of glucose and GOx in solution, the I_{pa}^{on}/I_{pa}^{off} ratio was 7.5, which is ~2 times larger than that in the absence of glucose and GOx for the system.
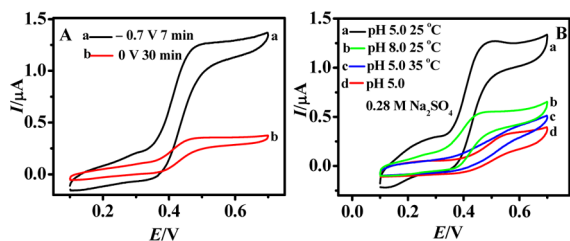
Figure 7. CV of 0.5 mM Fc(COOH)$_2$ at rGO/PNIPAA film electrodes at 0.01 V s^{-1} in buffers containing 6.0 mM glucose and 1.0 mg mL^{-1} GOx (A) at pH 8.0 after the films were treated at (a) −0.7 V for 7 min and (b) 0 V for 30 min at 25 °C; (B) after the films were treated at 0 V for 30 min at (a) 25 °C and pH 5.0, (b) 25 °C and pH 8.0, (c) 35 °C and pH 5.0, and (d) 25 °C and pH 5.0, with 0.28 M Na$_2$SO$_4$.

Similar amplification for the on−off CV behavior by the bioelectrocatalysis was also observed for the pH-, temperature-, and sulfate-sensitive system (Figure 7B). The multiple-stimuli switchable bioelectrocatalysis was found to be reversible and could be switched for many cycles (Figure S12 in the Supporting Information).

3.7. Logic Gate Circuit Based on the Multiple-Stimuli Switchable System.

The quadruply switchable bioelectrocatalysis system was employed to build a four-input logic gate circuit. In the present study, pH was considered as Input A with pH 8.0 and 5.0 as the "0" and "1" states, respectively; potential was defined as Input B, and 0 and −0.7 V were defined as the "0" and "1" states, respectively; temperature was considered as Input C with 35 °C and 25 °C as the "0" and "1" states, respectively; and the concentration of Na$_2$SO$_4$ was defined as Input D, where 0.28 and 0 M were defined as the "0" and "1" states, respectively. The I_{pa} of Fc(COOH)$_2$ for the rGO/PNIPAA films in buffers containing glucose and GOx was defined as the Output: the I_{pa} greater than 6 μA is considered as the "1" state, and the I_{pa} less than 6 μA is considered as the "0" state, with 6 μA as the threshold. There would be totally 16 possible combinations of the 4 inputs, and the combinations and the corresponding outputs are listed in the truth table (Table 2). Only the three input combinations (1,1,1,1; 1,0,1,1; and 0,1,1,1) led to the output "1" or the on state, while the

Table 2. Truth Table of the Four-Input Logic Gate Circuit for the System

Input A pH	Input B potential	Input C temperature	Input D [Na$_2$SO$_4$]	Output I_{pa}
1	1	1	1	1
1	0	1	1	1
0	1	1	1	1
0	0	1	1	0
1	1	0	1	0
0	1	0	1	0
1	0	0	1	0
0	0	0	1	0
1	1	1	0	0
1	0	1	0	0
0	1	1	0	0
0	0	1	0	0
1	1	0	0	0
0	1	0	0	0
1	0	0	0	0
0	0	0	0	0

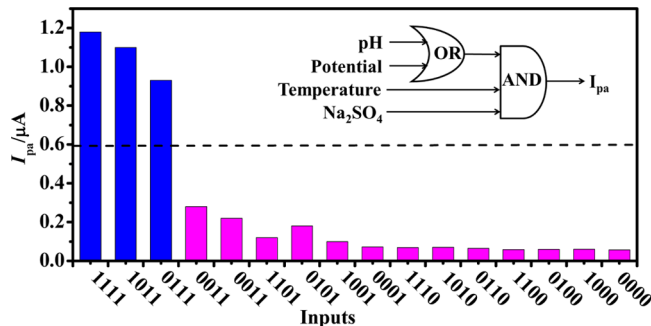other 13 input combinations correspond to the output "0" or the off state (Figure 8).

Figure 8. I_{pa} of 0.5 mM Fc(COOH)$_2$ for the rGO/PNIPAA films at 0.01 V s^{-1} in the buffer solution containing 6 mM glucose and 1.0 mg mL^{-1} GOx as the output, with all possible 16 combinations of the 4 inputs. The threshold is marked by dashed line. (inset) The symbolic representation of the logic gate circuit.

Note that the potential-responsive CV on−off property of the probe at the rGO/PNIPAA film electrodes could not be observed under the condition of pH 5.0. In other words, the system was always in the on state at pH 5.0, regardless of whether the film electrodes were treated by any potential. The potential-responsive property of this system could only be realized at pH 8.0. This unique behavior is in good agreement with an enabled OR (EnOR) logic gate circuit. That means, only when both Input C and Input D are activated to the "1" level, the gate can be enabled by either Input A or Input B at their "1" levels (Figure 8, inset).[9,55−57]

4. CONCLUSIONS

In this work, rGO/PNIPAA films are electrodeposited onto the surface of Au electrodes in less than 10 min. The probe Fc(COOH)$_2$ exhibits reversible potential-, pH-, thermo- and SO$_4^{2-}$-responsive CV on−off behavior at the rGO/PNIPAA film electrodes. The film system can also be used to realize multiple-stimuli switchable bioelectrocatalysis of glucose catalyzed by GOx and mediated by Fc(COOH)$_2$ in solution. The novel findings and breakthroughs of this work include: (1) the fast and "green" one-step electrodeposition method is used to synthesize the rGO/PNIPAA thin films on the electrode surface; (2) rGO is used as the sensitive component of the films to realize the multiswitchable bioelectrocatalysis; (3) the potential-responsive behavior of the system is based on the transformation between GO and rGO in the films at different potentials; and (4) the pH-sensitive property of the system is observed only after the films are treated at 0 V, thereby enabling the building of the unique EnOR logic gate with four inputs. At the present stage, this study just exhibits the proof-of-concept. However, it shows a significant step forward to the actual applications. For instance, this type of logic gate circuit can accept multiple inputs and lead to the binary output of YES/NO, which may be applied to some biomedical diagnosis.[9] This type of study may also settle the foundation for developing a new kind of intelligent decision-making logic network in biocomputing.

■ ASSOCIATED CONTENT

Ⓢ Supporting Information

Discussion of characterization of GO with IR and TEM. Table of the assignment of all of the characteristic IR absorption peaks of NIPAA, PNIPAA, rGO/PNIPAA, graphite, and GO samples. Twelve figures showing the IR spectra of the above-described samples, a TEM image of GO, the CV I_{pa} of $Fc(COOH)_2$ for rGO/PNIPAA films at different potentials, the CVs of $Fc(COOH)_2$ at PNIPAA electrodes after treatment at 0 V and −0.7 V, the CVs of $Fc(COOH)_2$ at the bare Au and PNIPAA electrodes at pH 5.0 and 8.0 after treatment at 0 V for 30 min, the CVs of FcOH, $Fe(CN)_6^{3-}$, and MB for rGO/PNIPAA films at different pH after treatment at 0 V for 30 min, the XPS spectra and the XPS profiles in the C 1s region for the PNIPAA, rGO/PNIPAA, and rGO films observed after treatments at different potentials, the CVs of $Fc(COOH)_2$ at different pH for rGO/PNIPAA films without treatment by the potentials, the concentration influence of Na_2SO_4, NaCl, and NaBr on the CV I_{pa} of $Fc(COOH)_2$ at pH 5.0 and 25 °C at the rGO/PNIPAA film electrodes, the CVs of $Fc(COOH)_2$ at 25 °C for the rGO/PNIPAA films in pH 5.0 buffers containing GOx and different concentration of glucose, the dependence of the CV I_{pa} of $Fc(COOH)_2$ for the same rGO/PNIPAA films in buffers containing GOx and glucose at 25 °C for the following cases: (1) when the solution pH switched between 5.0 and 8.0 after the films were treated at 0 V for 30 min, (2) in pH 8.0 buffers after the potential switched between −0.7 and 0 V, (3) in pH 5.0 buffers when the solution temperature switched between 25 °C and 35 °C, and (4) at pH 5.0 and 25 °C when the Na_2SO_4 concentration switched between 0 and 0.28 M. This material is available free of charge via the Internet at http://pubs.acs.org.

■ AUTHOR INFORMATION

Corresponding Author
*Phone: (86)-10-58807843. E-mail: liuhongyun@bnu.edu.cn.
Notes
The authors declare no competing financial interest.

■ ACKNOWLEDGMENTS

■ REFERENCES

(1) Wang, J.; Katz, E. Digital Biosensors with Built-in Logic for Biomedical Applications-Biosensors Based on a Biocomputing Concept. *Anal. Bioanal. Chem.* **2010**, *398*, 1591−1603.

(2) Willner, I.; Katz, E. Integration of Layered Redox Proteins and Conductive Supports for Bioelectronic Applications. *Angew. Chem., Int. Ed* **2000**, *39*, 1180−1218.

(3) Willner, I.; Katz, E. Magnetic Control of Electrocatalytic and Bioelectrocatalytic Processes. *Angew. Chem., Int. Ed* **2003**, *42*, 4576−4588.

(4) Antonio, T. R. T. A.; Cabral, M. F.; Cesarino, I.; Machado, S. A. S.; Pedrosa, V. A. Toward pH-Controllable Bioelectrocatalysis for Hydrogen Peroxide Based on Polymer Brushes. *Electrochem. Commun.* **2013**, *29*, 41−44.

(5) Song, S.; Hu, N. "On−Off" Switchable Bioelectrocatalysis Synergistically Controlled by Temperature and Sodium Sulfate Concentration Based on Poly (N-isopropylacrylamide) Films. *J. Phys. Chem. B* **2010**, *114*, 5940−5945.

(6) Katz, E.; Willner, I. A Biofuel Cell with Electrochemically Switchable and Tunable Power Output. *J. Am. Chem. Soc.* **2003**, *125*, 6803−6813.

(7) Willner, I.; Willner, B. Functional Nanoparticle Architectures for Sensoric, Optoelectronic, and Bioelectronic Applications. *Pure Appl. Chem.* **2002**, *74*, 1773−1783.

(8) Blonder, R.; Katz, E.; Willner, I.; Wray, V.; Bückmann, A. F. Application of a Nitrospiropyran-Fad-Reconstituted Glucose Oxidase and Charged Electron Mediators as Optobioelectronic Assemblies for the Amperometric Transduction of Recorded Optical Signals: Control of the "On"-"Off" Direction of the Photoswitch. *J. Am. Chem. Soc.* **1997**, *119*, 11747−11757.

(9) Liu, D.; Liu, H.; Hu, N. pH-, Sugar-, and Temperature-Sensitive Electrochemical Switch Amplified by Enzymatic Reaction and Controlled by Logic Gates Based on Semi-Interpenetrating Polymer Networks. *J. Phys. Chem. B* **2012**, *116*, 1700−1708.

(10) Liu, S.; Wang, L.; Lian, W.; Liu, H.; Li, C.-Z. Logic Gate System with Three Outputs and Three Inputs Based on Switchable Electrocatalysis of Glucose by Glucose Oxidase Entrapped in Chitosan Films. *Chem.—Asian J.* **2015**, *10*, 225−230.

(11) Zhang, K.; Liang, Y.; Liu, D.; Liu, H. An On-Off Biosensor Based on Multistimuli-Responsive Polymer Films with a Binary Architecture and Bioelectrocatalysis. *Sens. Actuators, B* **2012**, *173*, 967−976.

(12) Zhang, K.; Lian, W.; Liu, S.; Liu, H. Multi-Switchable Bioelectrocatalysis Based on Semi-Interpenetrating Polymer Network Films Prepared by Enzyme-Induced Polymerization. *J. Electrochem. Soc.* **2014**, *161*, H493−H500.

(13) Wang, J.; Katz, E. Digital Biosensors with Built-in Logic for Biomedical Applications. *Isr. J. Chem.* **2011**, *51*, 141−150.

(14) Strack, G.; Ornatska, M.; Pita, M.; Katz, E. Biocomputing Security System: Concatenated Enzyme-Based Logic Gates Operating as a Biomolecular Keypad Lock. *J. Am. Chem. Soc.* **2008**, *130*, 4234−4235.

(15) Wang, P.; Liu, S.; Liu, H. Multiple Stimuli-Switchable Bioelectrocatalysis under Physiological Conditions Based on Copolymer Films with Entrapped Enzyme. *J. Phys. Chem. B* **2014**, *118*, 6653−6661.

(16) Park, S.; Ruoff, R. S. Chemical Methods for the Production of Graphenes. *Nat. Nanotechnol.* **2009**, *4*, 217−224.

(17) Kim, F.; Cote, L. J.; Huang, J. Graphene Oxide: Surface Activity and Two-Dimensional Assembly. *Adv. Mater.* **2010**, *22*, 1954−1958.

(18) Cai, W.; Piner, R. D.; Stadermann, F. J.; Park, S.; Shaibat, M. A.; Ishii, Y.; Yang, D.; Velamakanni, A.; An, S. J.; Stoller, M.; An, J.; Chen, D.; Ruoff, R. S. Synthesis and Solid-State NMR Structural Characterization of (13)C-Labeled Graphite Oxide. *Science* **2008**, *321*, 1815−1817.

(19) Bai, H.; Li, C.; Wang, X.; Shi, G. A pH-Sensitive Graphene Oxide Composite Hydrogel. *Chem. Commun.* **2010**, *46*, 2376−2378.

(20) Liu, J.; Guo, S.; Han, L.; Ren, W.; Liu, Y.; Wang, E. Multiple pH-Responsive Graphene Composites by Non-Covalent Modification with Chitosan. *Talanta* **2012**, *101*, 151−156.

(21) Fang, M.; Long, L.; Zhao, W.; Wang, L.; Chen, G. pH-Responsive Chitosan-Mediated Graphene Dispersions. *Langmuir* **2010**, *26*, 16771−16774.

(22) Ren, L.; Liu, T.; Guo, J.; Guo, S.; Wang, X.; Wang, W. A Smart pH Responsive Graphene/Polyacrylamide Complex via Noncovalent Interaction. *Nanotechnology* **2010**, *21*, 16771−16774.

(23) Guo, H.-L.; Wang, X.-F.; Qian, Q.-Y.; Wang, F.-B.; Xia, X.-H. A Green Approach to the Synthesis of Graphene Nanosheets. *ACS Nano* **2009**, *3*, 2653−2659.

(24) Palenzuela, J.; Vinuales, A.; Odriozola, I.; Cabanero, G.; Grande, H. J.; Ruiz, V. Flexible Viologen Electrochromic Devices with Low Operational Voltages Using Reduced Graphene Oxide Electrodes. *ACS Appl. Mater. Interfaces* **2014**, *6*, 14562−14567.

(25) Sukhishvili, S. A. Responsive Polymer Films and Capsules via Layer-by-Layer Assembly. *Curr. Opin. Colloid Interface Sci.* **2005**, *10*, 37−44.

(26) Schild, H. G. Poly(N-isopropylacrylamide)-Experiment, Theory and Application. *Prog. Polym. Sci.* **1992**, *17*, 163−249.

(27) Katsumoto, Y.; Tanaka, T.; Sato, H.; Ozaki, Y. Conformational Change of Poly(N-isopropylacrylamide) During the Coil-Globule Transition Investigated by Attenuated Total Reflection/Infrared Spectroscopy and Density Functional Theory Calculation. *J. Phys. Chem. A* **2002**, *106*, 3429−3435.

(28) Deng, Y.; Zhang, J. Z.; Li, Y.; Hu, J.; Yang, D.; Huang, X. Thermoresponsive Graphene Oxide-PNIPAM Nanocomposites with Controllable Grafting Polymer Chains Via Moderate in Situ SET-LRP. *J. Polym. Sci.* **2012**, *50*, 4451−4458.

(29) Lo, C.-W.; Zhu, D.; Jiang, H. An Infrared-Light Responsive Graphene-Oxide Incorporated Poly(N-isopropylacrylamide) Hydrogel Nanocomposite. *Soft Matter* **2011**, *7*, 5604−5609.

(30) Li, Z.; Shen, J.; Ma, H.; Lu, X.; Shi, M.; Li, N.; Ye, M. Preparation and Characterization of pH- and Temperature-Responsive Hydrogels with Surface-Functionalized Graphene Oxide as the Crosslinker. *Soft Matter* **2012**, *8*, 3139−3145.

(31) Zhu, C.-H.; Lu, Y.; Peng, J.; Chen, J.-F.; Yu, S.-H. Photothermally Sensitive Poly(N-isopropylacrylamide)/Graphene Oxide Nanocomposite Hydrogels as Remote Light-Controlled Liquid Microvalves. *Adv. Funct. Mater.* **2012**, *22*, 4017−4022.

(32) Qi, J.; Lv, W.; Zhang, G.; Zhang, F.; Fan, X. Poly(N-isopropylacrylamide) on Two-Dimensional Graphene Oxide Surfaces. *Polym. Chem.* **2012**, *3*, 621−624.

(33) Pan, Y.; Bao, H.; Sahoo, N. G.; Wu, T.; Li, L. Water-Soluble Poly(N-isopropylacrylamide)-Graphene Sheets Synthesized via Click Chemistry for Drug Delivery. *Adv. Funct. Mater.* **2011**, *21*, 2754−2763.

(34) Hummers, W. S.; Offeman, R. E. Preparation of Graphitic Oxide. *J. Am. Chem. Soc.* **1958**, *80*, 1339−1339.

(35) Zhou, J.; Liu, J.; Wang, G.; Lu, X.; Wen, Z.; Li, J. Poly(N-isopropylacrylamide) Interfaces with Dissimilar Thermo-Responsive Behavior for Controlling Ion Permeation and Immobilization. *Adv. Funct. Mater.* **2007**, *17*, 3377−3382.

(36) Niyogi, S.; Bekyarova, E.; Itkis, M. E.; Zhang, H.; Shepperd, K.; Hicks, J.; Sprinkle, M.; Berger, C.; Lau, C. N.; deHeer, W. A.; Conrad, E. H.; Haddon, R. C. Spectroscopy of Covalently Functionalized Graphene. *Nano Lett.* **2010**, *10*, 4061−4066.

(37) Alzari, V.; Nuvoli, D.; Scognamillo, S.; Piccinini, M.; Gioffredi, E.; Malucelli, G.; Marceddu, S.; Sechi, M.; Sanna, V.; Mariani, A. Graphene-Containing Thermoresponsive Nanocomposite Hydrogels of Poly (N-isopropylacrylamide) Prepared by Frontal Polymerization. *J. Mater. Chem.* **2011**, *21*, 8727−8733.

(38) Shen, J.; Hu, Y.; Shi, M.; Lu, X.; Qin, C.; Li, C.; Ye, M. Fast and Facile Preparation of Graphene Oxide and Reduced Graphene Oxide Nanoplatelets. *Chem. Mater.* **2009**, *21*, 3514−3520.

(39) Stankovich, S.; Dikin, D. A.; Piner, R. D.; Kohlhaas, K. A.; Kleinhammes, A.; Jia, Y.; Wu, Y.; Nguyen, S. T.; Ruoff, R. S. Synthesis of Graphene-Based Nanosheets via Chemical Reduction of Exfoliated Graphite Oxide. *Carbon* **2007**, *45*, 1558−1565.

(40) Motornov, M.; Sheparovych, R.; Katz, E.; Minko, S. Chemical Gating with Nanostructured Responsive Polymer Brushes: Mixed Brush Versus Homopolymer Brush. *ACS Nano* **2007**, *2*, 41−52.

(41) Kang, E.-H.; Liu, X.; Sun, J.; Shen, J. Robust Ion-Permselective Multilayer Films Prepared by Photolysis of Polyelectrolyte Multilayers Containing Photo-Cross-Linkable and Photolabile Groups. *Langmuir* **2006**, *22*, 7894−7901.

(42) Calvo, A.; Yameen, B.; Williams, F. J.; Soler-Illia, G. J.; Azzaroni, O. Mesoporous Films and Polymer Brushes Helping Each Other to Modulate Ionic Transport in Nanoconfined Environments. An Interesting Example of Synergism in Functional Hybrid Assemblies. *J. Am. Chem. Soc.* **2009**, *131*, 10866−10868.

(43) Benito, A.; Martínez-Máñez, R.; Soto, J.; Tendero, M. J. L. Predicting the Maximum Oxidation Potential Shift in Redox-Active pH-Responsive Molecules in Their Electrostatic Interaction with Substrates. *J. Chem. Soc., Faraday Trans.* **1997**, *93*, 2175−2180.

(44) Woodward, R.; Rosenblum, M.; Whiting, M. A New Aromatic System. *J. Am. Chem. Soc.* **1952**, *74*, 3458−3459.

(45) Zhang, X.-F.; Shao, X.; Liu, S. Dual Fluorescence of Graphene Oxide: A Time-Resolved Study. *J. Phys. Chem. A* **2012**, *116*, 7308−7313.

(46) Shao, Y.; Wang, J.; Engelhard, M.; Wang, C.; Lin, Y. Facile and Controllable Electrochemical Reduction of Graphene Oxide and its Applications. *J. Mater. Chem.* **2010**, *20*, 743−748.

(47) Katsumoto, Y.; Tanaka, T.; Sato, H.; Ozaki, Y. Conformational Change of Poly (N-isopropylacrylamide) During the Coil-Globule Transition Investigated by Attenuated Total Reflection/Infrared Spectroscopy and Density Functional Theory Calculation. *J. Phys. Chem. A* **2002**, *106*, 3429−3435.

(48) Prevot, M.; Déjugnat, C.; Möhwald, H.; Sukhorukov, G. B. Behavior of Temperature-Sensitive PNIPAM Confined in Polyelectrolyte Capsules. *ChemPhysChem* **2006**, *7*, 2497−2502.

(49) Choi, Y.-J.; Yamaguchi, T.; Nakao, S.-I. A Novel Separation System Using Porous Thermosensitive Membranes. *Ind. Eng. Chem. Res.* **2000**, *39*, 2491−2495.

(50) Annaka, M.; Motokawa, K.; Sasaki, S.; Nakahira, T.; Kawasaki, H.; Maeda, H.; Amo, Y.; Tominaga, Y. Salt-Induced Volume Phase Transition of Poly(N-isopropylacrylamide) Gel. *J. Chem. Phys.* **2000**, *113*, 5980−5985.

(51) Junk, M. J. N.; Anac, I.; Menges, B.; Jonas, U. Analysis of Optical Gradient Profiles During Temperature- and Salt-Dependent Swelling of Thin Responsive Hydrogel Films. *Langmuir* **2010**, *26*, 12253−12259.

(52) Panayiotou, M.; Freitag, R. Influence of the Synthesis Conditions and Ionic Additives on the Swelling Behaviour of Thermo-Responsive Polyalkylacrylamide Hydrogels. *Polymer* **2005**, *46*, 6777−6785.

(53) Wang, J. Electrochemical Glucose Biosensors. *Chem. Rev.* **2008**, *108*, 814−825.

(54) Alzari, P.; Anicet, N.; Bourdillon, C.; Moiroux, J.; Saveant, J. M. Molecular Recognition of Artificial Single-Electron Acceptor Cosubstrates by Glucose Oxidase. *J. Am. Chem. Soc.* **1996**, *118*, 6788−6789.

(55) Roque, A.; Pina, F.; Alves, S.; Ballardini, R.; Maestri, M.; Balzani, V. Micelle Effect on the "Write-Lock-Read-Unlock-Erase" Cycle of 4′-Hydroxyflavylium Ion. *J. Mater. Chem.* **1999**, *9*, 2265−2269.

(56) de Sousa, M.; de Castro, B.; Abad, S.; Miranda, M. A.; Pischel, U. A Molecular Tool Kit for the Variable Design of Logic Operations (NOR, INH, EnNOR). *Chem. Commun.* **2006**, 2051−2053.

(57) Kahan-Hanum, M.; Douek, Y.; Adar, R.; Shapiro, E. A Library of Programmable DNAzymes that Operate in a Cellular Environment. *Sci. Rep.* **2013**, *3*, 1535 DOI: 10.1038/srep01535.